CO3D Image Quality Calibration

Fabrice Buffe[1], Sylvain Lucas[1], Alice Latourte[1], Nicolas Delaygue[1], Timothée Accadia[1], David Youssefi[1], Arthur Dick[1], Clément Luitot[1], Mickaël Bruno[1], Clément Coggiola[1], Yannick Tanguy[1], Laurent Lebègue[1], Colin Thomas[2], Marc Schillinger[2], Alice Chambrelan[2]

[1]Centre National d'Etudes Spatiales (CNES), 18 avenue E. Belin, 31400 Toulouse cedex 9, France
[2]Airbus Defense and Space, 31 Rue des Cosmonautes, 31400 Toulouse, France

CO3D session

Keywords: CO3D, Image Quality, Radiometry, Geometry, 3D, Calibration

Abstract

The launch of the four CO3D satellites took place on 25th July 2025. One of the goals of the mission is to generate a worldwide, accurate and low-cost Digital Surface Model (DSM) at a resolution and relative height accuracy of 1m. This 3D performance relies on well-controlled image quality: the radiometry and resolution ensure a performant matching between the stereo images, and the geometry guarantees an accurate altimetry. The Image Quality In-Orbit Test (IOT) phase has permitted to tune the on-board parameters before starting the massive acquisitions. Dedicated acquisition modes were used on calibration sites spread throughout the world. Thanks to the agility of the satellite, celestial acquisitions are possible and support the radiometry and resolution calibrations. This paper does not include the in-orbit performances due to confidentiality agreement.

1. Introduction

Since mid-2019, Airbus Defense & Space in partnership with CNES, is developing a new High Resolution Optical EO mission dedicated to very high resolution 3D observation called CO3D ("Constellation Optique 3D"). CO3D mission is based on a constellation of four optical satellites (Lebègue, 2020) acquiring images at a resolution of 50cm (Lebègue, 2026).

Images are acquired in red/green/blue (RGB) and near infra-red (NIR) spectral bands with a 50 cm Ground Sampling Distance (GSD), thanks to matrix sensors based on a Bayer pattern. This brings new calibration challenges compared to previous push broom systems (Pleiades, Pleiades-Neo …) such as demosaicing and 2D line of sight (LOS) geometrical determination.

The launch of the four CO3D spacecrafts took place on 25th July 2025 aboard Vega-C from Kourou space center together with the Microcarb microsatellite. After a first week spent calibrating the most critical subsystems of the platform, the instrument was switched on, enabling the 9-month Image Quality In-Orbit Test (IOT) phase to begin. At the end of the IOT, the spatial segment is verified as calibrated and the worldwide acquisitions can start. While raw data are beginning to arrive, the image processing chain CODIP (Melet, 2020) can still be adjusted for the next four months before the start of the massive production of the worldwide DSM.

2. In-Orbit Test overview

2.1 Calibration activities timeline

Calibration activities began a few days after launch, once the first images were performed. These activities were organized to calibrate the satellites and evaluate their performance as quickly as possible, while taking into account the mission's significant constraints: calibration of four satellites, numerous calibration steps and numerous performance metrics to be evaluated (from instruments characteristics to 3D products precision). The key highlights of the first months of IOT are described in Figure 1.

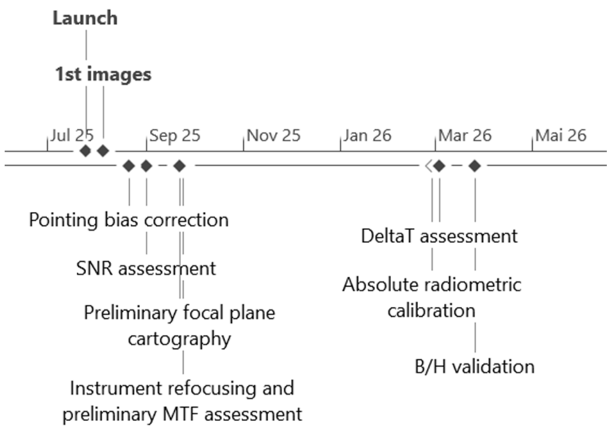

Figure 1 : Key elements of the IOT

2.2 In-orbit test organization

The calibration activities take places on a cloud-based infrastructure called Image Calibration Center (ICC). It enables the definition and sending of acquisitions requests by managing several interfaces with the Airbus ground segment. It also hosts computing resources for calibration processing and catalogs the images and the processing parameters (Melet, 2026).

The Image Quality team is made up of engineers from CNES and Airbus Defense & Space and has gathered for 9 months at the CNES office where the ICC is located. The team consists of about 20 people working on radiometry, resolution, geometry and 3D activities. IGN (Institut National Geographique) is also implicated in the IOT by supporting the global block adjustment and 3D qualification activities. The exploitation team, consisting of three people and located in the same room, handles the submission of acquisition requests and manages routine processes which guaranty that the performances are stable in the exploitation phase. The ICC development team is located in an adjacent office and provides daily support to the Image Quality team.

3. Radiometric Activities

All radiometric activities are performed for both visible (VIS) and near-infrared (NIR) sensors. Bayer processing typically involves decomposing the color planes to assess the red, green and blue bands individually. For some metrics, discrepancies between these bands provide a confidence interval for the assessment.

3.1 On-board and ground normalization

Among the standard activities of radiometric calibration, detector normalization is important because it delivers uniform images of uniform areas. This normalization is processed on board to mitigate the downlink rate. Unlike the Pleiades system, the dark and offset normalization tables cannot be loaded via the upstream link due to their size, which corresponds to a 150-million-pixel matrix sensor. Specific on-board processing and guidance maneuvers have been developed for this purpose.

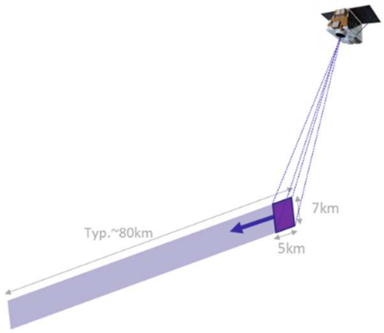

Figure 2. CO3D drifting summation acquisition process. 100 images are acquired along an 80km-long strip and summed. On-board stacking of successive acquisitions over different sites is possible.

On-board offset and gain creation is based on a drifting guidance combined while directly summing several images. For gain tables, this is performed over landscapes as uniform as possible like Antarctica or deserts. Even if this acquisition mode should average the scenery across the sensor, some residue might remain. Therefore, we stack on-board several summations acquired over different areas of interest. Offset tables use summation acquisitions over dark oceans at night, far from the coasts to avoid any light source. Equalization tables are directly computed on-board, based on those summed acquisitions.

	Specification	Applicability
HF residue	<0.5%	95% of 50x50 pix.
LF residue	<5%	All pixels
Structured noise	<1% white noise	99.7% pixels
Defective pixels	<0.1%	All pixels

Table 1. CO3D radiometric specification related to equalization, with the associated stringency. The defective pixel specification is understood before processing while equalization residues are evaluated after.

Table 1 lists CO3D equalization specification. They are linked to the potential low (LF) / high frequency (HF) residues after equalization and structured noise. The latter might appear due to image downlink effects, electromagnetic coupling effects or remaining electronic chain spurious or readout artefacts.

Due to ageing components, some pixels may not respond normally to incident light over time. We call them defective if they are too noisy, appear black in highlights or white in shadows, or if their response is non-linear. Even if there is only a negligible amount, without correction, those pixels may contaminate the neighbouring area during interpolation steps such as Bayer demosaicing. These pixels are detected using summation acquisition and interpolated during the normalisation process. Night images are acquired with longer integration time compared to daylight images. Some defects are then appearing due to this acquisition configuration change, that are not visible on daylight images. Thus, dedicated corrections are applied to remove them, which needs to be configured differently compared to daylight acquisitions. As illustrated in Figure 3, these pixels are mostly visible in low-radiance areas.

Figure 3. CO3D demosaiced night image of Istanbul acquired with a 70ms integration time, before (left) and after (right) defective pixels interpolation.

3.2 Integration time tuning and Signal-to-noise ratio assessment

CO3D uses state-of-the-art matrix sensors. In addition to their many radiometric qualities, such as low noise and integrated colour filters, the acquisition's integration time can be tailored to ensure an optimal signal-to-noise ratio (SNR). The sun's zenith angle (SZA), which varies with latitude and season, directly impacts the input radiance at the instrument level by roughly the factor cos(SZA). To comply with 3D global specifications, a good, uniform SNR is required for all acquisitions worldwide. The CO3D system adapts its integration time to the local SZA to ensure compliance with the SNR specification. This is why the CO3D system is more sensitive in shadows and at high latitudes than traditional push-broom satellites. The integration time model as a function of SZA was consolidated and validated during IOT.

	SNR @L1	MTF	FoM
R @50cm	25	0.05	1.5
G @50cm	30	0.05	1.5
B @50cm	30	0.05	1.5
NIR @1m	40	0.05	1.5

Table 2. Radiometric and resolution specification expressed in terms of SNR, MTF (Modulation Transfer Function) and figure of merit (FoM). SNR specification is given here at L1 radiance, where it is the most stringent. FoM is the product of SNR and MTF, this specification ensures a good image quality if one of the SNR or MTF specification is not met.

Theoretical SNR evaluation is based on noise model measurement. Dark temporal and spatial noise are evaluated in flight. As summation acquisitions are not compressed, they are also used to assess the instrument spatial noise (the on-board sum

This contribution has been peer-reviewed.
https://doi.org/10.5194/isprs-archives-XLIX-B1-2026-523-2026 | © Author(s) 2026. CC BY 4.0 License.

averages the temporal noise). CO3D SNR assessment relies on massive automatic processing over random landscapes acquired during IOT. SNR specification can be found in Table 2. CO3D performs well in terms of SNR especially at low radiance. This ensures a good radiometric content in the shadows and at high latitude, supporting 3D reconstruction in dense urban areas.

Details over CO3D noise and SNR assessment techniques and the associated performances can be found in (Lucas, 2026).

3.3 Absolute Calibration activities

Absolute calibration activities aim at updating the radiometric model parameters (gain and offset for CO3D) to convert numerical counts of the image into radiometric quantities (radiance) and also monitoring these parameters over time. It also helps the generation of the land cover mask in the image processing chain (Tanguy, 2024). Two methods are combined to calibrate and monitor the absolute radiometry.

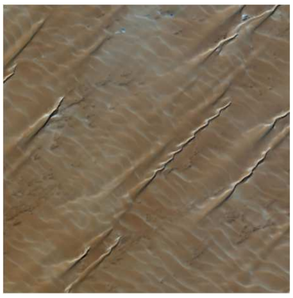

Figure 4 : Lybia_1 by CO3D, used for the absolute calibration

Figure 5 : Moon acquired by CO3D

The Pseudo-Invariant Calibration Sites (PICS) method cross-calibrate CO3D measures with high-quality measures from reference sensors over desertic sites, known for the stability of their Bottom of Atmosphere (BOA) reflectance (Figure 6).

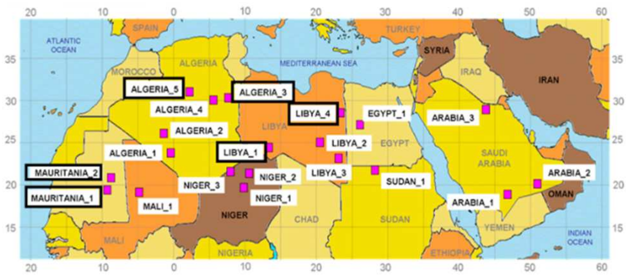

Figure 6 : Desert PICS used for the CalVal CO3D activities. Black boxes are the 6 PICS recommended by CEOS.

Since 1982, the CNES has developed the SADE/MUSCLE system to perform such cross-calibrations (Alhammoud, 2025). The SADE database now contains more than 33 million of reference measures (mean image radiances) over the different PICS. The MUSCLE software allows us to select those with a similar geometry of acquisition than the CO3D ones. It uses a Radiative Transfer Model (RTM) to propagate these reference Top of the Atmosphere (TOA) radiances back to the surface, then spectrally interpolate them into the CO3D spectral bands and finally propagate them again at TOA level where they can be compared with the CO3D measures to cross-calibrate.

First comparisons made between the four CO3D satellites using the on-ground radiometric coefficients and OLCI-B as reference sensors show a very good agreement (Figure 7). Even if those results demonstrate good pre-flight measurement, current IOT calibrations will deliver better performance.

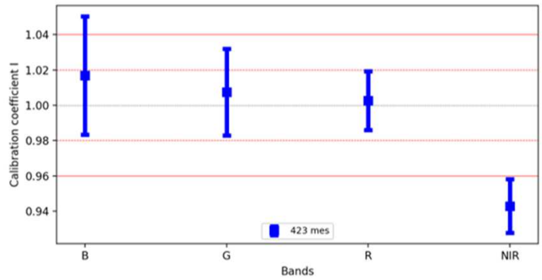

Figure 7 : Ratio between CO3D and OLCI-B (reference sensor) TOA reflectances. This demonstrates a really good pre-flight calibration: better than 4% (VIS band) and better than 6% (NIR)

The Moon Calibration method is used here to monitor the time-evolution of the radiometric parameters. Measured lunar irradiance is compared with a modeled one. The model is derived from the Robotic Lunar Observatory (ROLO) from USGS (United States Geological Survey) considering the VIS + NIR corrections proposed by CNES using PEIADES images (Meygret, 2017). The agility of the CO3D spacecraft is used to take several images of the Moon during an orbit. From these images, an integrated measure of the Moon irradiance is computed for each spectral band, based on the on-ground radiometric parameters of the instruments. The positions of the Sun and the satellite in the selenocentric frame are used as inputs for the ROLO-CNES model to compute the same integrated lunar irradiance and to compare it to the measure.

4. Resolution Activities

The main activities are dedicated to the instrument refocus and the MTF (Modulation Transfer Function) measurement. After initial IOT activities, monitoring compression rates ensures that the system will be able to download all the expected data during the bulk acquisition phase.

4.1 Datasets

In the same way as was done on Pleiades, images on stars were mainly used. CO3D can acquire bursts of images, as illustrated by Figure 8 of both terrestrial and celestial targets. Despite the shear potential number of frames, those acquisitions are not compressed for ground transmission, preserving the full range of instrumental effects in the images. Similar uncompressed bursts were acquired on selected ground targets to simulate the compression/decompression process.

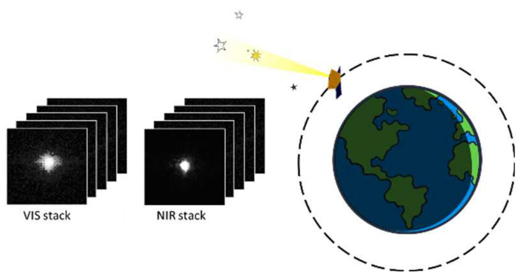

Figure 8. CO3D star burst acquisitions principle. The satellite can do a series of such acquisition in a single orbit. This allows gathering data stacks over multiple areas of the sensors in a short time frame.

The stars were selected to ensure a strong enough signal for the four blue, green, red and near-infrared bands with a standard integration time (Lucas, 2023). Stars with companions or optical doubles were rejected to ensure imaging of a single light source within the frame. The list of the remaining available stars is given in Table 3

Star name	HIP index	Magnitude
Alpha Ursae Minoris	HIP_11767	1.97
Pi^3 Orionis	HIP_22449	3.19
Zeta Hydrae	HIP_43813	3.11
Epsilon Leonis	HIP_47908	2.97
Epsilon Virginis	HIP_63608	2.85
Epsilon Ophiuchi	HIP_79882	3.23
Eta Serpentis	HIP_89962	3.23
Delta Draconis	HIP_94376	3.07
Beta Aquarii	HIP_106278	2.9

Table 3. CO3D compatible stars list acquired during IOT.

4.2 Refocus operations

Refocusing operations have been conducted soon after launch thanks to several methods. We primarily used star stacks acquired under different thermal settings and processed using a phase diversity algorithm (Latry, 2017). This provides both the defocus value and a detailed evaluation of all the optical aberrations contributing to the wavefront error (WFE), projected on the Zernike polynomial basis. For each thermal setting, urbans areas were acquired for visual comparison and empirical evaluation of the defocus.

Additional measurements and control where performed, based on point-spread function (PSF) full width at half maximum (FWHM) evaluation and PSF super-resolution as described in (Lucas, 2026). Those four methods provided a thermal setting best focus estimate with an averaged dispersion for all satellites and bands σ_{Z_4} lower than 15nm (expressed as WFE defocus).

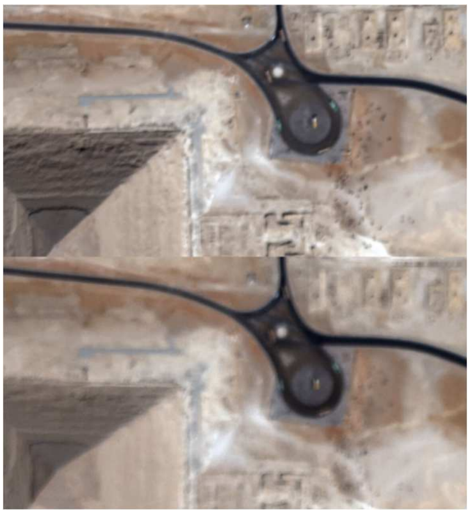

Figure 9. First CO3D1 (Top) / CO3D2 (Bottom) synchronous acquisition, Gizah pyramids, before any instrument refocus operation. Both instruments were out of focus.

Figure 9 shows the initial defocus of the first two satellites before any dedicated operation. These instruments were focused one month after launch. The two others were in focus soon after their commissioning phase and before the end of September.

4.3 MTF assessment

Based on super-resolved PSF and phase diversity outputs, we could assess precisely the instrument static MTF, including both sensor attenuation and optical aberrations. These static MTF measurements form the basis for generating the ground deconvolution filters. They are applied during the restoration process in the image processing chain and consist in reverting the instrument low-path filter effects. CO3D MTF evaluation and restoration is detailed in (Lucas, 2026).

Dynamic effects were assessed on terrestrial acquisition based on geometric modelling and AOCS (Attitude and Orbit Control Subsystem) measurements. Those include platform stability (drift and vibration) and guidance induced footprint distortion during imaging time and they all vary linearly with the integration time (T_i). This is inconsistent with the varying integration time strategy implemented to maintain a constant SNR, which increases in ration of $\sqrt{T_i}$.

Thus, a trade-off is necessary between MTF and SNR performance. This is the reason for the figure of merit (FoM) specification given in Table 2, with FoM being the product of MTF and SNR. Consequently, the implemented Ti law as a function of SZA balances both SNR and MTF needs. CO3D SNR & MTF performance are assessed at satellite level, without any processing. Ground restoration makes up for instrumental effects: radiometric processing denoises the images and increases their sharpness.

4.4 Compression monitoring

Once the radiometry has been calibrated, the precise onboard compression bit rate can be monitored and the quality target is fined-tuned to match the mission requirements.

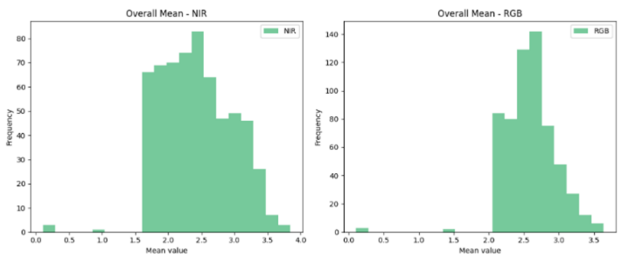

Tableau 1: Extract over a few weeks of CO3D NIR (left) and RGB (right) mean bit rates.

CO3D on-board image compression is based on a CNES quality-driven compression algorithm (Camarero, 2012). This algorithm allows a user to obtain a local specific quality target on each 8x8 block in the wavelet domain. This target, denoted k, is defined as a fraction of the local noise level (Cucchetti, 2021).

During IOT the compression calibration consists in the acquisition of multiple raw uncompressed images from various landscapes in order to test multiple quality settings. From one raw image, one can generate compressed/decompressed images, with a different quality setting each. This allows comparing the impact of compression on the image weight depending on the quality. Classical image quality metrics could be monitored (for example: Mean Square Error with respect to the instrumental noise, SNR) however because the human visual perception does not rely well on mathematical metrics, a visual analysis is performed on the images to spot the areas, landscapes or details where compression loss is visible.

By the end of IOT, from the analysis of various landscapes (deserts, forests, dense cities, shores, etc.), the perfect balance between quality, bandwidth and visual artifacts will be set in order to get the best quantity and quality of images from CO3D.

5. Geometric Activities

5.1 Geo-location calibration

During the first weeks in IOT, a rough bias has been corrected on board which permits to enhance the pointing error by a factor of five (Erblang, 2026). This pitch and roll correction has been performed by taking manual measurements on Google Earth. It was a prerequisite for acquisitions needed for other calibration activities, such as moon and stars images for radiometry and resolution. This made it possible to run the automatic matching process on SRP (Space Reference Points, Chandelier, 2020) on several hundred of products. This extensive data set permits after 3 months to refine the pitch and roll on-board correction by a factor of three and to correct the yaw angle.

Works are on-going to reduce the Absolute Pointing Error (APE) by highlighting dependencies on orbital parameters. For this purpose, Nadir acquisitions distributed along the orbit are determined through an automated process that takes the weather into account.

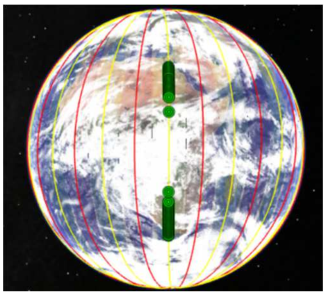

Figure 10 : example of one orbit dedicated to bias measurement where acquisitions are planned where the weather permits

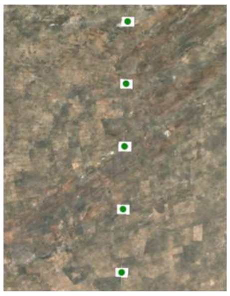

Figure 11 : zoom of a portion of this orbit where acquisitions are evenly spaced

These corrections improve the overlap area between two adjacent scenes (see Figure 28 for a mosaic illustration). It also reduce the exploration area in CODIP process of SRP matching which is essential to reach the planimetric requirement of 5m expected on the processed products.

5.2 Multi-spectral registration

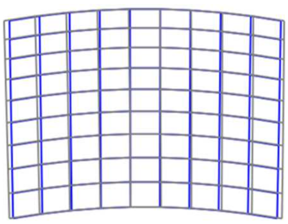

Blue: ground projection of RGB sensor
Grey: ground projection of NIR sensor

Figure 12 : ground projection of line of sight with an amplified deformation for a better visualization

Early in the IOT, it is crucial to demonstrate the capability of delivering images with a performant overlay between the spectral bands. The red, blue and green are natively registered thanks to a unique bayer sensor. On the other hand, the Near Infra-red band is acquired by a seperate sensor. By design, the NIR footprint is slightly larger than the RGB one (see Figure 12).

A model of the difference between RGB and NIR lines of sight must be established to enable the resampling in a common geometry (perfect sensor, ortho-image) with a good superposition between the spectral bands (requirement set to 0.3 pixels). It is a prerequisite for image compositions (see Figure 14) and land cover masks calculation (Tanguy, 2024 and Youssefi, 2026).

Figure 13 : RGB imagery

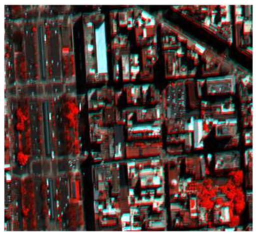

Figure 14 : colored composition with the NIR represented in red

This relative model is established by image correction techniques (normalized cross correlation or mutual information) between NIR and green @50cm. The accuracy of the result is compromised by contrast inversion, particularly on vegetation which reflects a lot of signal in NIR wavelength. This effect is illustrated in Figure 15 and Figure 16 with a clear distinction on the disparity map created by the landscape: the trees are mostly located in the upper part of the image.

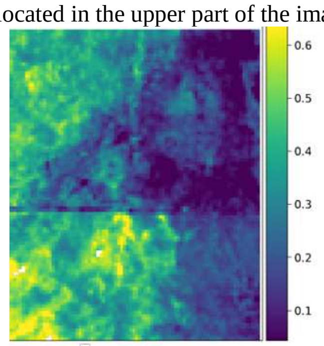

Figure 15 : Disparity map from matching between green and NIR

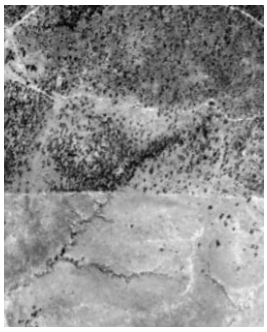

Figure 16 green corresponding image

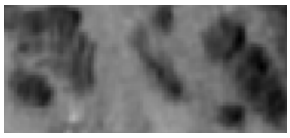

Figure 17 : Zoom on trees in the green band

Figure 18 : Zoom on trees in the NIR band

To reduce the measurement noise, hundreds of images were processed using automatic filters to remove those which are the most impacted by the contrast inversion. Some new techniques are envisaged to make the NIR-RGB correlation more robust, i.e. Channel Features of Oriented Gradients (Ye, 2019) or by filtering ambiguous correlation (Sarrazin, 2021). The NIR-RGB geometric calibration relies on a specific acquisition tuning. To ensure a perfect synchronization between the NIR and RGB acquisitions, the integration times are set to the same value and the two acquisitions start simultaneously. Otherwise, the starting time of the NIR acquisition can be shifted up to 30ms (DeltaT, see Figure 19). It helps the attitude estimation (see part 5.4). The

Integration time (Ti) can be set differently for RBG and NIR sensors (see part 3).

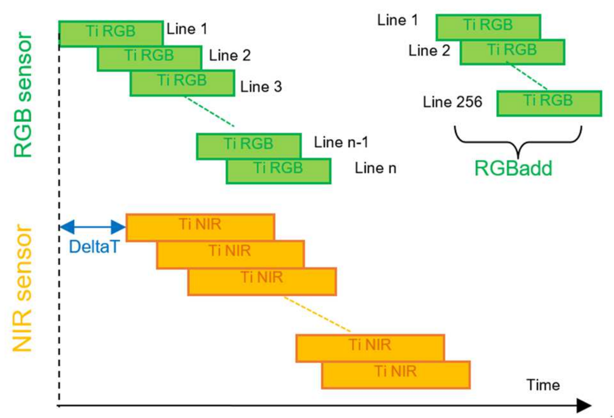

Figure 19 : NIR and RGB acquisition principles. The RGBadd is dedicated to the attitude drift restitution

5.3 Focal plane cartography

The distortion correction is an activity that is carried out on missions where a precise geometric accuracy is essential. The requirement on the knowledge of lines of sight is set at 0.1 pixels to mitigate the contribution to the altimetry budget. The purpose of this activity is to establish an absolute angular model that restitutes the distortion as shown on the grey ground projection on Figure 12.

Unlike Pleiades satellites, CO3D has matrix sensors that requires a specific method based on line of sight (LOS) auto-calibration (Vidal, 2022). The auto-calibration is convenient for high-resolution imagery: it mitigates the correlation between attitude errors and line of sight. The various incidence angles (pitch and roll) add sufficient constraints without having a precise reference DSM. It offers the possibility to select various calibration sites without having precise references and thus allows other criteria to be prioritized: well textured and stable landscape, good weather, no conflict with other calibration sites.

Figure 20 : Location of LOS calibration sites

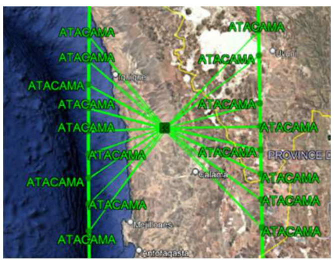

Figure 21 : 18 acquisition accesses on a LOS calibration site from two different orbits

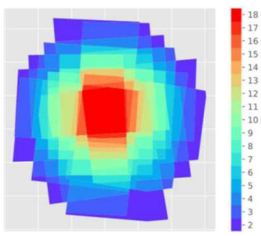

Figure 22 : overlapping ground footprints of 18 acquisitions used for line-of-sight calibration

Eighteen overlapping images are acquired on each site with varying acquisition angles (Figure 22). Starting with the 18-acquisition group, a LOS model is established based on a spatio-triangulation process. For one satellite, a dozen of LOS models are calculated from each site (Laurent, 2026). The auto-calibration allows establishing a LOS model up to a rotation and a scaling factor (Figure 23). The models are thus compared between sites after compensation of a yaw tilt and a magnification and the standard deviation between them is the final validation criteria. The retained model corresponds to the average of all models.

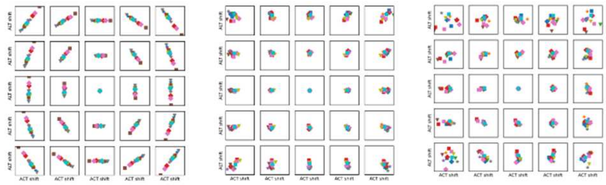

Figure 23 : comparison between the LOS models on 5 x 5 locations of the field of view of the same satellite: without tilt compensation (left), without magnification compensation (middle), with both compensation (right). Each color corresponds to a same LOS model. Each dot represents an offset in row / column.

The tilt is systematically corrected in CODIP thanks to the unitary refinement based on SRP. The magnification may be corrected in CODIP thanks to the global spatio-triangulation (Erblang 2026). It is also calibrated by stacking the magnifications measured on hundreds of images to reduce the unitary SRP matching noise.

5.4 Line-of-sight dynamic stability

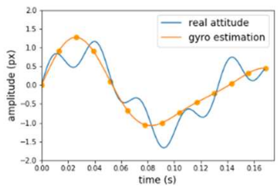

Figure 24: Comparison of a simulated attitude profile with vibrations and simulated gyro measurement which is representative of the low frequencies (Buffe, 2024)

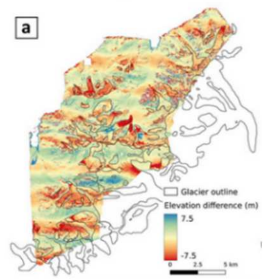

Figure 25: Effect of a vibration on a DSM (Berthier, 2024)

Geometric calibration is a prerequisite to achieve the targeted 3D performance. Vibrations on the attitude profile induce altimetric oscillation on DSM (see Figure 25). The requirement is set to 0.1 pixels. Innovative correction methods have been prepared before launch combining gyrometer measurement and multispectral bands correlation (Buffe, 2024). Observation on flight images prompts an adjustment of the method. Nevertheless, the NIR/RGB matching remains the key feature to correct the satellite attitude thanks to the shift between the start dates of RGB and NIR (DeltaT see Figure 19). Different shifts have been tested in IOT to find an optimal value. A final check is performed at the DSM qualification step to ensure there are no residues due to satellite attitude jitter.

Figure 26 : portion of one orbit where double acquisitions are evenly spaced

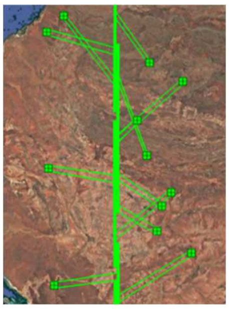

Figure 27 : portion of one orbit where acquisitions with various incidence angles are planned

Different acquisition modes that may affect the satellite attitude profiles are explored: double acquisitions with two different satellite maneuvers (see Figure 26) and various incidence angles within the flight envelope (see Figure 27).

5.5 Global block adjustment tuning

A global block adjustment, gathering around 100 different CO3D images, is carried out which insures a good geometrical coherency between the adjacent product (Melet, 2020). It mitigates the altimetric shift between adjacent unitary DSM after the 3D merging.

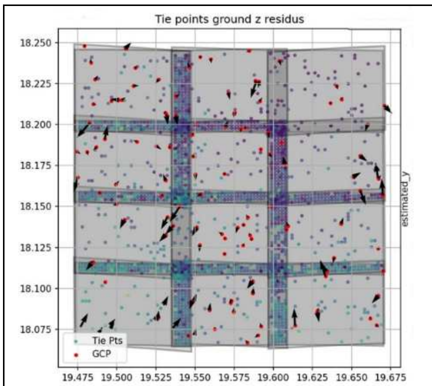

Figure 28: block adjustment measures corresponding to a 3 x 4 stereo pairs (~ 20x20 km^2) on Tchad qualification site

Different measures are combined in the global block adjustment (Erblang, 2026):
- Ground control point (SRP) with a planimetric and altimetric constraints. The Z measures of SRP is the main driver of the DSM absolute altimetry performance (red dots on Figure 28).
- Tie points that link between two images and eight images which improve the geometric consistency between adjacent products (blue/purple dots on Figure 28)

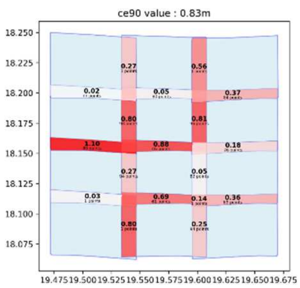

Figure 29: Altimetric gap on overlap areas on Tchad before parameters tuning

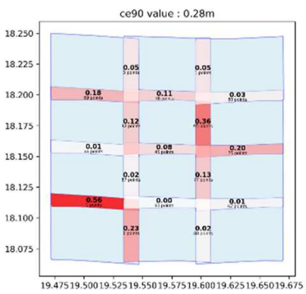

Figure 30: Altimetric gap on overlap areas on Tchad after parameters tuning

A higher density of tie points on overlap areas provides a better constraint on the altimetric gap between adjacent DSM. Thanks to an optimized tuning achieved with the help of IGN, these gaps are mitigated (see Figure 29 and Figure 30). The requirement is set to 0.6m. The final check is performed at the DSM qualification step (see part 6.1).

6. 3D Activities

3D activities take place in a second stage of the commissioning phase once radiometric and geometric calibration are finalized. This includes the verification of the altimetry performances that constitutes a main requirement of the CO3D mission (Lebegue, 2024) and the validation of the DSM quality which is a key criterion for product users. These activities are mainly carried out during the first few months following the start of the massive acquisitions (Youssefi, 2026). Two specific activities that are directly linked to the altimetry performance are highlighted in this paper.

6.1 Global block adjustment validation

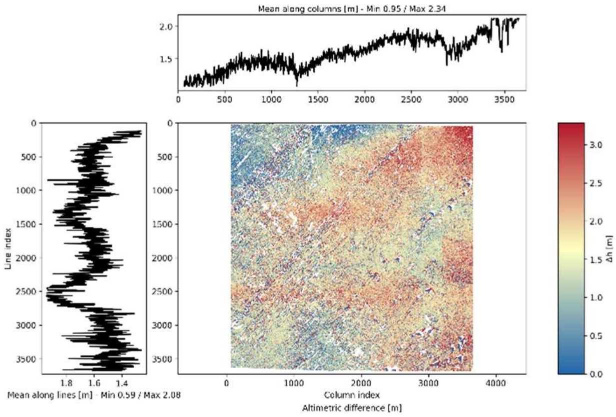

Figure 31: global block adjustment validation on Tchad

In collaboration with IGN, CO3D DSM are qualified with respect to reference model based on Pleiades-Neo Imagery (see Figure 31). In particular, this makes it possible to quantify the residues from the global block-adjustment process. Works are ongoing to extend this qualification process to larger mosaics up to L4 standard-sized distribution products.

6.2 B over H ratio tuning

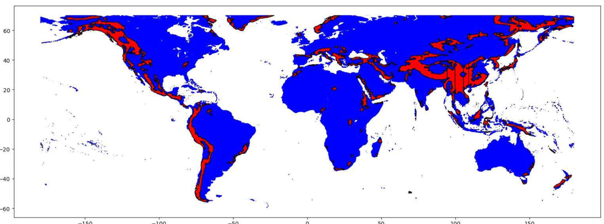

Figure 32: B/H world map

The B over H ratio (B/H) is a key factor of the DSM performance. The higher B/H is, the better the altimetry performance but number of occlusions increases. A compromise is set before the start of massive acquisitions. The world map is divided into two parts: B/H = 0.3 for moderate slope in blue and B/H = 0.2 for high relief in red (see Figure 32). By testing different B/H values in IOT on dedicated qualification sites, the two values are adjusted before the start of the massive acquisitions.

Acknowledgements

The author would like to thank the whole team of image experts who have performed a great job, spending time, energy and enthusiasm during the 9 months of IOT. He would also like to thank the CODIP/ICC team for its support and the exploitation team for their constant good mood, providing the experts with acquisitions and image products.

References

Alhammoud B., Desjardin C., Sterckx S., Adriaensen S., Mackenzie C., Bourg L., Clerc S. Dransfeld S., Copernicus Sentinel-3 OLCI Level-1B Radiometry Product Validation Status After Six Years in Constellation by Three Independent Expert Groups, Remote Sensing 2025, 17(7), 1217, https://doi.org/10.3390/rs17071217

Berthier, E., Lebreton, J., Fontannaz, D., Hosford, S., Belart, J. M.-C., Brun, F., Andreassen, L. M., Menounos, B., and Blondel, C.: The Pléiades Glacier Observatory: high-resolution digital elevation models and ortho-imagery to monitor glacier change, The Cryosphere, 18, 5551–5571, https://doi.org/10.5194/tc-18-5551-2024, 2024

F. Buffe, G. Laurent, B. Mamdy and C. L’Helguen, "Attitude Restitution of Earth Observation Satellites by Coupling AOCS Measurement and Multispectral Correlation," *IGARSS 2024 - 2024 IEEE International Geoscience and Remote Sensing Symposium*, Athens, Greece, 2024, pp. 6420-6424, doi: 10.1109/IGARSS53475.2024.10642591

Camarero, Roberto & Delaunay, Xavier & Thiebaut, Carole. (2012). Fixed-Quality/Variable bit-rate On-Board Image Compression for future CNES missions. Proceedings of SPIE - The International Society for Optical Engineering. 8514. 851402. 10.1117/12.928965

Chandelier, L., Coeurdevey, L., Bosch, S., Favé, P., Gachet, R., Orsoni, A., Tilak, T., and Barot, A.: A WORLDWIDE 3D GCP DATABASE INHERITED FROM 20 YEARS OF MASSIVE MULTI-SATELLITE OBSERVATIONS, ISPRS Ann. Photogramm. Remote Sens. Spatial Inf. Sci., V-2-2020, 15–23, https://doi.org/10.5194/isprs-annals-V-2-2020-15-2020, 2020

Cucchetti, E., Latry, C., Blanchet, G., Delvit, J.-M., and Bruno, M.: ONBOARD/ON-GROUND IMAGE PROCESSING CHAIN FOR HIGH-RESOLUTION EARTH OBSERVATION SATELLITES, Int. Arch. Photogramm. Remote Sens. Spatial Inf. Sci., XLIII-B3-2021, 755–762, https://doi.org/10.5194/isprs-archives-XLIII-B3-2021-755-2021, 2021

Erblang, M. Saulnier, E. Laurent, G. Delaygue, N. Buffe, F. Latourte, Alice; Jassaud, M. Bricout, N. 2026: Global Block Adjustment for Mosaicked Stereoscopic Satellite, ISPRS 2026, Toronto (submitted)

Latry, C. Delvit, J.M. Thiebaut, Carole. Sensitivity analysis of phase diversity technique for high resolution earth observing telescopes. ICSO 2017. Proc. of SPIE Vol. 10562 105623X-1

Laurent, G., Latourte, L. Buffe, F. Vidal, B. 2026: Line Of Sight Calibration For Satellite Imagery Based On Matrix Detector, ISPRS 2026, Toronto (submitted)

L. Lebègue, E. Le-Hir, F. Buffe, P. Favé, D. Youssefi and A. Lombard, "CO3D Products Qualification Forecast," *IGARSS 2024 - 2024 IEEE International Geoscience and Remote Sensing Symposium*, Athens, Greece, 2024, pp. 8555-8559, doi: 10.1109/IGARSS53475.2024.10640872

Lebègue, L., Buffe, F. Melet, O., Youssefi D., Henry, J.B. 2026: The CO3D mission, a worldwide one-meter accuracy Digital Surface Model, ISPRS 2026, Toronto (submitted)

Lucas, S. Amram, O. Latry, C. Thomas, C. Schillinger, M. 2026: Radiometric features and ground processing for high-resolution Earth observation satellite Bayer matrix-based images like CO3D, ISPRS 2026, Toronto (submitted)

Melet, O., Youssefi, D., David, L’Helguen, C., Michel, J., Sarrazin, E., Languille, F., Lebegue, L., 2020. Co3d mission digital surface model production pipeline. ISPRS - International Archives of the Photogrammetry, Remote Sensing and Spatial Information Sciences

Melet, O. L'Helguen, C. Pradines, L. Youssefi, D. Bellet, V. 2026: CNES CO3D Image Ground Segment, ISPRS 2026, Toronto (submitted)

Meygret, A.; Blanchet, G.; Colzy, S.; Gross-Colzy, L. Improving ROLO lunar albedo model using PLEIADES-HR satellites extra-terrestrial observations. In Proceedings of Earth Observing Systems XXII; SPIE: San Diego, CA, USA, 2017; Volume 10402, p. 104022A.

Sarrazin, E., Cournet, M., Dumas, L., Defonte, V., Fardet, Q., Steux, Y., Jimenez Diaz, N., Dubois, E., Youssefi, D., and Buffe, F.: AMBIGUITY CONCEPT IN STEREO MATCHING PIPELINE, Int. Arch. Photogramm. Remote Sens. Spatial Inf. Sci., XLIII-B2-2021, 383–390, https://doi.org/10.5194/isprs-archives-XLIII-B2-2021-383-2021, 2021

Y. Tanguy, C. Raille and F. Buffe, "Smart Land Use Masks : A Simple and Robust Approach to Produce Low/High Vegetation Masks from a Single High Resolution Satellite Image," *IGARSS 2024 - 2024 IEEE International Geoscience and Remote Sensing Symposium*, Athens, Greece, 2024, pp. 4164-4168, doi: 10.1109/IGARSS53475.2024.10641347

Vidal, B., Laurent, G., Buffe, F., Binet, R., Zanga, W., and Greslou, D.: LINE OF SIGHT AUTO-CALIBRATION FOR CO3D ROLLING SHUTTER MATRIX DETECTOR, Int. Arch. Photogramm. Remote Sens. Spatial Inf. Sci., XLIII-B1-2022, 107–112, https://doi.org/10.5194/isprs-archives-XLIII-B1-2022-107-2022, 2022

Ye, Y., Bruzzone, L., Shan, J., Bovolo, F., & Zhu, Q. (2019). Fast and robust matching for multimodal remote sensing image registration. *IEEE Transactions on Geoscience and Remote Sensing*, *57*(11), 9059-9070.

Youssefi, D. Accadia, T. Colleu, E. Godet, A. Bellet, V. Lallement, D. Tanguy, Y. Lebegue, L. 2026: 3D Product Quality Control in the CO3D Mission: A Critical Role, ISPRS 2026, Toronto (submitted)